applied sciences

MDPI

Article

Engineering Properties and Microscopic Mechanisms of Composite-Cemented Soil as Backfill of Ultra-Deep and Ultra-Narrow Foundation Trenches

Xu Dong [1], Mingdong Wang [1], Minyuan Song [1,2] and Ning Hou [1,*]

[1] School of Civil Engineering, Shandong Jiaotong University, Jinan 250357, China
[2] Shandong Railway Investment Holding Group Co., Ltd., Jinan 250357, China
* Correspondence: sdhouning@163.com

Abstract: The backfilling of lime soil in ultra-deep and ultra-narrow foundation trenches is a difficult construction link, and ordinary-cemented soil has drawbacks, including poor strength, impermeability, and frost resistance. To solve these problems, fly ash (FA)–water glass (WG)-composite-cemented soil is developed based on a background project. The three-factor orthogonal tests are conducted on the unconfined compressive strength (UCS) of the composite-cemented soil, and the optimal engineering mix proportion is proposed for the FA-WG-composite-cemented soil. Its UCS is compared with that of cemented soil only doped with FA or WG (FA- and WG-cemented soil). In addition, the cyclic wetting–drying tests, cyclic freeze–thaw tests, and impermeability tests are carried out to study the endurance of the composite-cemented soil in cold regions rich in water. The hydration products of the composite-cemented soil are investigated through scanning electron microscopy (SEM) and X-ray diffraction (XRD) analysis, and the curing mechanism of the composite-cemented soil is discussed from the microscopic perspective. The research results indicate that the mixing ratio of cement is crucial to the strength development of the cemented soil; the mixing ratio of FA greatly influences the strength development of the cemented soil in the middle and late stages; the mixing ratio of WG only slightly affects the strength. The ratio of cement, FA, and WG of 9%:12%:3% is the optimal engineering mix proportion of the composite-cemented soil. Compared with ordinary-cemented oil and FA- and WG-cemented soil, the composite-cemented soil shows significantly improved compressive load-bearing capacity. The permeability coefficient of the composite-cemented soil is always obviously lower than that of the ordinary-cemented soil after any curing period. Despite the mass loss, the composite-cemented soil is superior to the ordinary one in overall endurance after wetting–drying and freeze–thaw cycles. Through SEM and XRD analysis, the content of hydration products of the composite-cemented soil is found to be obviously higher than that of ordinary-cemented soil after any curing period, and the hydrates exert stronger cementing action on soil particles in the composite-cemented soil. The contents of C-S-H gel and Aft crystals in the composite-cemented soil are apparently larger than those in the ordinary-cemented soil. Under the alkali activation of WG, the FA produces free SiO_3^{2-} and AlO^{2-}, which undergo the polymerization reaction with Ca^{2+} to generate C-S-H gel and C-A-H gel, further promoting the hydration of cement.

Keywords: foundation trench; composite-cemented soil; unconfined compressive strength; impermeability; endurance; microscopic property; curing mechanism

check for updates

Citation: Dong, X.; Wang, M.; Song, M.; Hou, N. Engineering Properties and Microscopic Mechanisms of Composite-Cemented Soil as Backfill of Ultra-Deep and Ultra-Narrow Foundation Trenches. *Appl. Sci.* **2023**, *13*, 1952. https://doi.org/10.3390/app13031952

Academic Editor: Eduardo Garzon

Received: 10 January 2023
Revised: 27 January 2023
Accepted: 30 January 2023
Published: 2 February 2023

Copyright: © 2023 by the authors. Licensee MDPI, Basel, Switzerland. This article is an open access article distributed under the terms and conditions of the Creative Commons Attribution (CC BY) license (https://creativecommons.org/licenses/by/4.0/).

1. Introduction

With the rapid development of urbanization, lots of high-rise buildings and buildings in underground spaces are constructed due to restrictions on land use in cities. Correspondingly, the foundation pits of these buildings are also dug increasingly deeper. Meanwhile, the construction of foundation pits faces many problems because of the complexity and sensitivity of use functions of the buildings, narrow construction space, and complex construction environment [1,2]. Foundation trenches are the spaces between the foundation

and retaining walls of foundation pits. Because foundation pits are dug deeper and deeper, the foundation trenches are increasingly narrower. For some deep foundation pits, the width of foundation trenches is even less than one meter. The backfill materials and backfilling methods of foundation trenches are of important significance for the overall stability of the buildings, the normal use of pipelines, and the safety of foundations [3,4].

The backfilling method commonly used in engineering is to backfill and compact 2:8 lime soil in layers [5,6]. In engineering practice, the method is found to have some drawbacks: Firstly, the compaction in layers needs compacting equipment, while large compacting machinery is not applicable to narrow foundation trenches, so artificial compaction can only be adopted. This causes low construction efficiency and delays the construction schedule. Secondly, compacted lime soil has a low load-bearing capacity, so the method is not suitable for special buildings that have requirements for load-bearing capacity. Thirdly, lime soil is not waterproof [7], so a large volume of retained water exists in foundation trenches, which applies huge additional pressure on the basement walls. Therefore, special waterproofing work needs to be conducted for underground structures of buildings, which substantially increases the overall cost of buildings.

Cemented soil is a hard material of special engineering properties formed by mixing, vibrating, and curing the mixture composed of soil as the aggregate, Portland cement as the cementing material, and water as the reaction medium, and it is also termed as cement-stabilized soil [8–10]. Cemented soil is widely used in fields including roadbeds, canal lining and slope protection in water conservancy projects, and foundation reinforcement of buildings [11,12]. Its economic, social, and environmental benefits have been long confirmed. However, engineering practice also finds that the strength and impermeability of cemented soil are closely related to the cement content, and cemented soil has high strength at room temperature, while its strength is greatly deteriorated under conditions of freeze–thaw cycles [13–15]. How to improve the strength, impermeability, and frost resistance of cemented soil, on the premise of ensuring the economic efficiency of the use amount of cemented soil, is the key to further promoting the application of cemented soil in cold regions rich in water [16,17]. An effective measure to improve the strength of cemented soil is to dope additives to improve the compactness of structures [18–20]. Therefore, selecting an appropriate additive has become an important topic to improve the strength and endurance of cemented soil and also a research hot spot of researchers in China and abroad [21–27]. In such contexts, the concept of composite-cemented soil is emergent.

Aiming at shortcomings of ordinary-cemented soil, the fly ash (FA)–water glass (WG)-composite-cemented soil material was developed based on a background project. The unconfined compressive strengths (UCS) of ordinary-cemented soil and cemented soil only doped with FA and WG (FA- and WG-cemented soil) were tested. The orthogonal test schemes for the UCS of the composite-cemented soil were established, and the contents of cement, FA, and WG were selected as variables to study the UCS of the composite-cemented soil after different curing periods. The results were compared with the UCS of ordinary-cemented soil and FA- and WG-cemented soil to further propose the optimal mix proportion of the FA-WG-composite-cemented soil. The endurance of the composite-cemented soil in cold regions rich in water was studied by conducting cyclic wetting–drying tests, cyclic freeze–thaw tests, and impermeability tests. Through scanning electron microscopy (SEM) and X-ray diffraction (XRD) analysis, the curing mechanism of the composite-cemented soil was discussed from the microscopic perspective.

2. Project Characteristics and Material Properties

2.1. Project Characteristics

The transportation hub project of the south square of a railway station mainly involves the south and north underground parking lots and the reversed rail transit project. It is designed to have two underground stories, and three underground stories in some areas. The total building area is about 1.4×10^5 m^2, and the foundation pit is 10~23 m deep.

The ramp bridges are on two sides of the underground parking lots, with a total length of 1575 m (Figure 1). The foundation pit is supported with composite-soil-nailed walls and pile anchors.



Figure 1. Construction site.

The backfilling of the foundation trenches faces the following difficulties: (1) The small backfilling spaces. The foundation trench in the south basement has the smallest bottom width of 1.5 m and a depth of 11 m; the bottom width and depth of the foundation trench in the north basement and rail transit are 1.5 m and 10~15 m, respectively. The backfilling space is so small that large equipment cannot be used for compaction. (2) The very large backfill volume. According to the approved support and precipitation design schemes of the foundation pit, the backfill volumes in the south and north basements as well as the rail transit are 2.5×10^4, 9.5×10^4, and 5×10^4 m^3, respectively, amounting to 1.7×10^5 m^3. (3) The tight schedule requirements. According to the construction progress, the project owner has set the schedule for the nodal project that backfilling of the foundation pit of the south underground parking lot should be finished within 60 d. (4) High requirement for backfilling quality. The load-bearing capacity in the backfilling range of the foundation pit should not be lower than that of undisturbed soil. There are abundant groundwater and high groundwater levels in the whole area of parking lots, so the waterproofing work of the main structure is the key and difficult point of the whole project. To solve the above problems, the composite-cemented soil was innovatively used in the project to backfill ultra-deep and ultra-narrow foundation trenches, as shown in Figure 2.



Figure 2. Casting and backfilling of composite-cemented soil.

2.2. Material Properties

2.2.1. Soil Samples

Undisturbed soil was excavated in the construction site of the foundation pit according to the test demand. Tests on the basic physical properties of soil samples include tests on the moisture content of natural soil, moisture content of air-dried soil, natural unit weight, and limited moisture content. The test results are listed in Table 1.

Table 1. Physical parameters of test soil samples.

Moisture Content of Natural Soil (w)	Moisture Content of Air-Dried Soil (w_0)	Natural Unit Weight (γ)	Plastic Limit (w_P)	Liquid Limit (w_L)	Plasticity Index (I_P)	Lithology
31.5%	4.0%	17.55 KN/m^3	21.5%	30.7%	9.2	Silty sand

A sample prepared with a small amount of soil was placed in a Bruker D8 Advance X-ray diffractometer for phase analysis. The XRD pattern of the plain soil is shown in Figure 3.

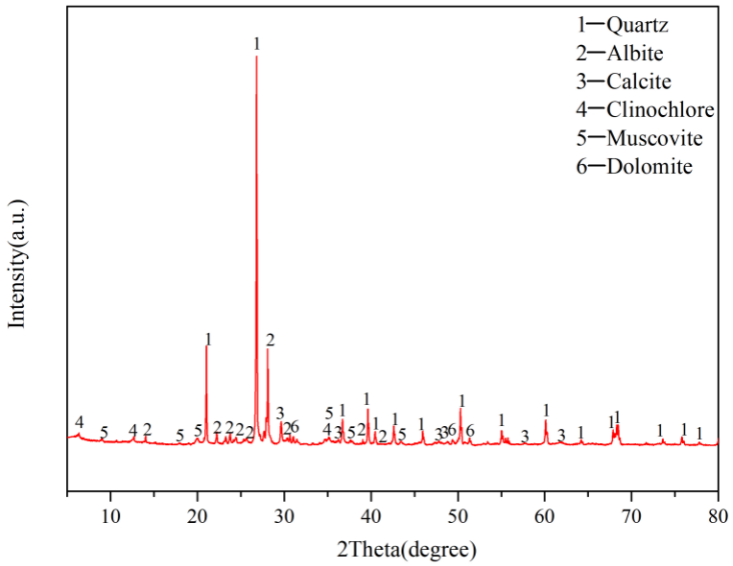


Figure 3. XRD pattern of a soil sample.

Comparing Figure 3 with the standard pattern reveals that the plain soil sample is mainly composed of quartz, muscovite, albite, and clinochlore, each of which corresponds to the abundant characteristics of the XRD pattern. This indicates the high crystallinity of each phase. According to the Scherrer equation, D_{hkl} is inversely proportional to β, and the XRD pattern exhibits a small full width at half maxima, so the sample has a relatively large average grain size. At the same time, Rietveld semi-quantitative phase analysis (RQPA) was carried out to determine the relative contents of each mineral. The semi-quantitative analysis data are shown in Table 2.

Table 2. The semi-quantitative analysis results based on XRD.

Composition	Quartz	Albite	Calcite	Clinochlore	Muscovite	Dolomite
	%	%	%	%	%	%
Content	46.5	13.8	1.4	7.2	29.2	1.9

2.2.2. Cement

The cement used in the test was PO42.5 ordinary Portland cement, whose main compositions and property indexes are shown in Table 3.

Table 3. Main compositions of PO42.5 ordinary Portland cement (%).

Chemical Compositions	CaO	SiO_2	Al_2O_3	MgO	SO_3	Fe_2O_3
Content %	51.42	24.99	8.26	3.71	2.51	4.03

2.2.3. FA

FA used in the tests was fine ash captured in the smoke emitted from a power plant due to the combustion of coal. FA is the main solid waste of coal-burning power plants, and its main compositions are provided in Table 4.

Table 4. Main compositions of FA (%).

Compositions	SiO_2	Al_2O_3	CaO	SO_3	Moisture Content	Loss on Ignition
Content %	45.1	24.2	5.6	2.1	0.85	4.7

2.2.4. WG

WG, commonly known as sodium silicate, is a kind of water-soluble silicate composed of alkali metal oxides and silicon dioxide. It has dual properties of solution and colloid and is, therefore, a complex colloidal solution. According to the different types of alkali metal oxides, WG is mainly divided into sodium and potassium ones. It is generally a colorless viscous liquid. In civil engineering, sodium WG is generally used (same in the tests). Two important parameters of WG include the module (n in the molecular formula of sodium WG, that is, the molar ratio of SiO_2 to Na_2O) and the Baume degree (the content or concentration of WG in an aqueous solution). The larger the module and Baume degree are, the higher the viscosity and strength of WG. Parameters and compositions of WG are provided in Table 5.

Table 5. Parameters and compositions of WG.

Molecular Formula	Baume Degree (20 °C)	Module (n)	SiO_2	Na_2O	$Na_2O.3.3SiO_2$
$Na_2O.nSiO_2$	38.5	3.3	27.45%	8.54%	35%

3. Tests on the Optimal Mix Proportion of Composite-Cemented Soil

3.1. Test Methods and Results

Orthogonal tests were carried out to analyze the influences of three factors, including contents of cement, FA, and WG, on the UCS of the FA-WG-composite-cemented soil and determine its optimal mix proportion. The tests were conducted on cylindrical samples measuring Φ50 mm × H50 mm [28], and the orthogonal test design and test results are listed in Table 6.

Table 6. UCS of the FA-WG-composite-cemented soil (MPa).

Group	Factor A	Factor B	Factor C	UCS/MPa		
				7 d	28 d	60 d
1	A1	B1	C1	1.63	3.51	4.06
2	A1	B2	C3	1.50	3.95	5.12
3	A1	B3	C2	2.22	4.41	5.62
4	A2	B1	C3	2.56	4.32	5.51
5	A2	B2	C2	3.10	4.66	5.67
6	A2	B3	C1	3.12	4.76	6.25
7	A3	B1	C2	3.54	6.09	7.41
8	A3	B2	C1	3.67	6.02	7.61
9	A3	B3	C3	4.33	6.35	8.20

Notes: Factor A is mixing ratio of cement, A1—6%, A2—9%, A3—12%. Factor B is mixing ratio of FA, B1—4%, B2—8%, B3—12%. Factor C is mixing ratio of WG, C1—1%, C2—3%, C3—5%.

Through range analysis and comprehensive analysis of variance of orthogonal test data, the mixing ratio of cement is crucial to the strength development of the cemented soil after any curing period; the mixing ratio of FA obviously influences the strength development of the cemented soil in the middle and late stages; and the mixing ratio of WG only slightly affects the strength. The theoretical optimal mix proportion is A3B3C2. Whereas considering the engineering application, a cement content of 9% is enough to meet the corresponding engineering requirements for backfilling of the deep foundation pit, that is, the ratio of cement, FA, and WG for FA-WG-composite-cemented soil is 9%:12%:3% under the optimal mix proportion.

3.2. Comparative Analysis

The UCS of the FA-WG-composite-cemented soil, ordinary-cemented soil, FA-cemented soil, and WG-cemented soil was compared to test their properties. The mix proportions of these four types of cemented soil are listed in Table 7, and the comparison results are illustrated in Figure 4.

Table 7. Mix proportions of the four types of cemented soil.

Type	Mixing Ratio of Cement	Mixing Ratio of FA	Mixing Ratio of WG
Ordinary-cemented soil	9%	0%	0%
FA-cemented soil	9%	12%	0%
WG-cemented soil	9%	0%	3%
Composite-cemented soil	9%	12%	3%

It can be seen from Figure 4 that the growth rate of the strength of the four types of cemented soil shows a similar pattern, and the strength of the cemented soils after being cured for 28 d is substantially improved compared with that after 7 d; the strength still approximately linearly grows after 28 d, while the growth rate declines greatly compared with that before 28 d. After each curing period, the composite-cemented soil always shows the highest strength, which indicates that co-doping of FA and WG exerts a remarkable effect in improving the strength of cemented soil. The strength of WG-cemented soil after being cured for 28 d is slightly higher than that of the FA one. This implies that WG has a more obvious effect on improving the strength of the cemented soil in the early stage; afterward, the FA-cemented soil is obviously superior to the WG one in terms of strength, indicating that doping of FA has an obvious effect on improving the strength of the cemented soil in the middle and late stages.

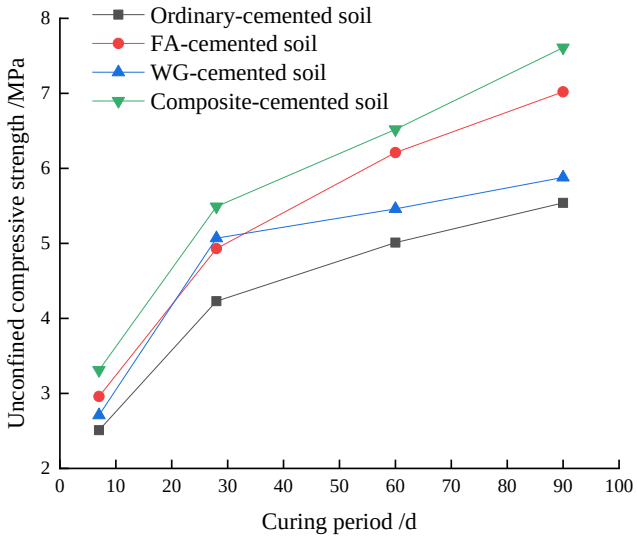


Figure 4. Changes of the UCS of the four types of cemented soil with the curing period.

4. Endurance of Composite-Cemented Soil

4.1. Impermeability Tests

Ordinary and composite-cemented soil samples with 9% of cement were prepared. The samples were truncated conical samples obtained by artificial vibration and molding in layers, measuring Φ_{upper} 70 mm × Φ_{lower} 80 mm × H30 mm. In the tests, the permeability coefficients of the ordinary- and composite-cemented soil cured for 7, 28, and 60 d were measured. The test results are displayed in Figure 5.

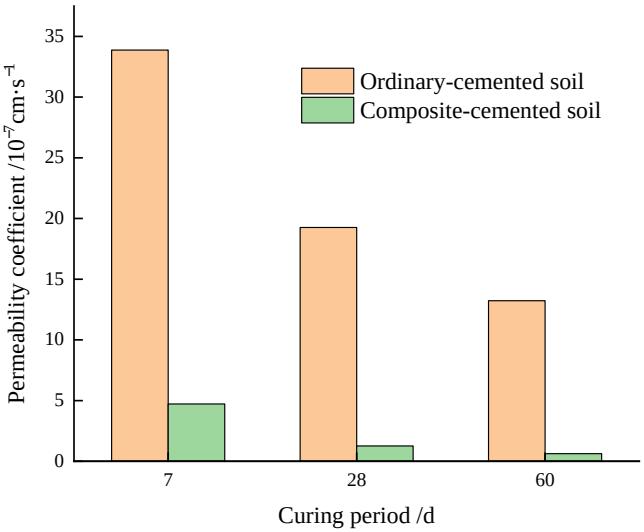


Figure 5. Comparison of permeability coefficients of different types of cemented soil after different curing periods.

It can be seen from Figure 5 that the permeability coefficient of the composite-cemented soil is always significantly lower than that of ordinary-cemented soil after different curing periods. This is because the reactions of the additives in the composite-cemented soil, that is, the active reaction of FA and the catalytic reaction of WG, both consume the hydration product $Ca(OH)_2$ when other conditions are the same. This produces calcium silicate hydrate (C-S-H) while promoting the hydration reaction of cement. The large amounts of hydration products are aggregated on the surface of soil particles and fill in the pores

between soil particles, rendering the composite-cemented soil with more compact soil structures than the ordinary one, so the impermeability is greatly improved.

4.2. Cyclic Wetting–Drying and Freeze–Thaw Tests

Samples of the ordinary and composite-cemented soil both with a cement content of 9% were prepared in the tests. The samples with the dimensions of Φ50 mm × H50 mm were statically compacted and cured for 28 d. The tests involved two parallel test groups, that is, one group was subjected to wetting–drying cycles and the other to freeze–thaw cycles. The ordinary- and composite-cemented soil samples were separately subjected to 4, 8, 12, and 16 wetting–drying and freeze–thaw cycles following the standard test methods [28]. The surface damage of the samples subjected to wetting–drying cycles is shown in Figure 6, and that of samples after freeze–thaw cycles is illustrated in Figure 7.

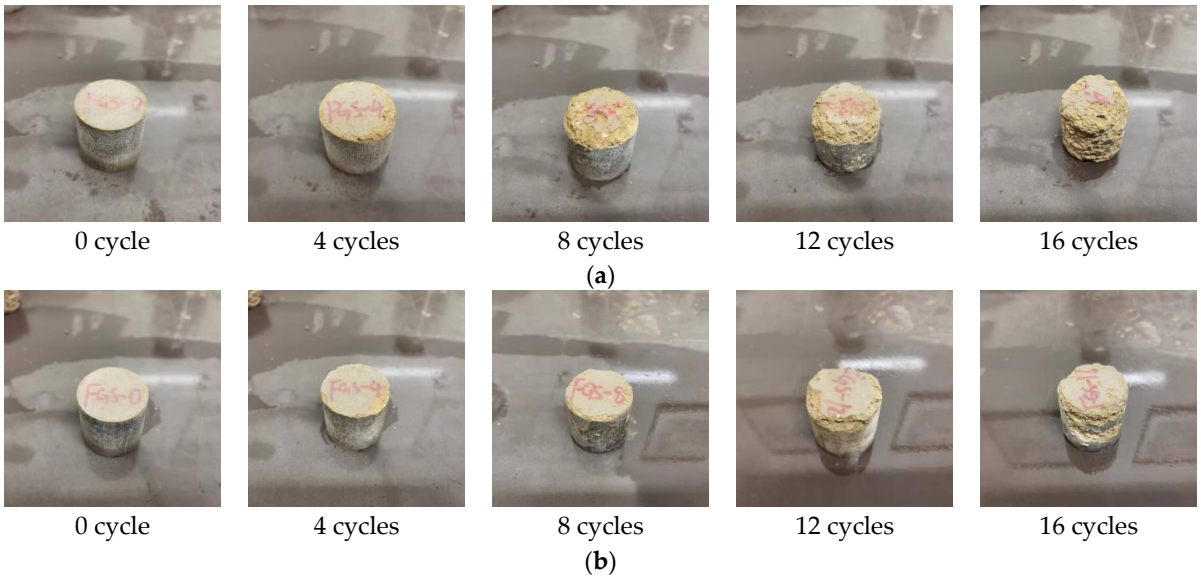


Figure 6. (**a**) Damage of ordinary-cemented soil subjected to wetting–drying cycles (cured for 28 d). (**b**) Damage of composite-cemented soil subjected to wetting–drying cycles (cured for 28 d).

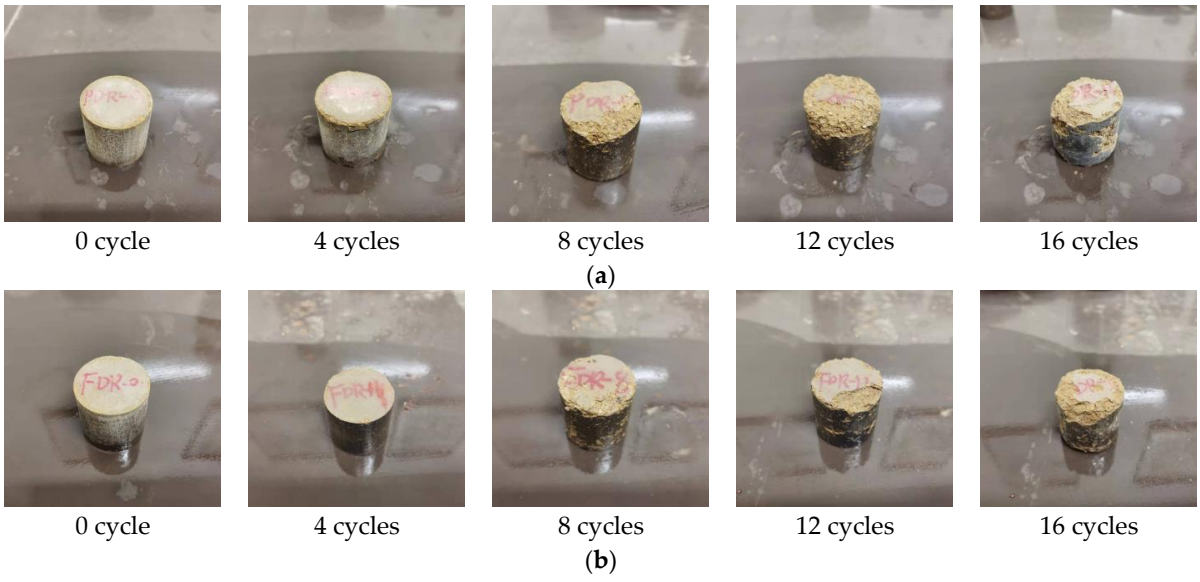


Figure 7. (**a**) Damage of ordinary-cemented soil subjected to freeze–thaw cycles (cured for 28 d). (**b**) Damage of composite-cemented soil subjected to freeze–thaw cycles (cured for 28 d).

As shown in Figure 6, the edges of the ordinary and composite-cemented soil samples are both chipped and lost, and their outer walls are eroded after 8 wetting–drying cycles; after 16 wetting–drying cycles, pits and slots spread all over the samples. However, the comparison indicates that the ordinary-cemented soil has a larger mass loss after wetting–drying cycles, while the composite-cemented soil has a higher resistance to wetting–drying cycles than the ordinary one. It can be seen from Figure 7 that damage, including chipped and lost edges, eroded outer walls, and widespread pits and slots, is also observed on ordinary and composite-cemented soil after freeze–thaw cycles. Similarly, the ordinary-cemented soil also shows a larger mass loss after freeze–thaw cycles, which indicates that the composite-cemented soil is of higher resistance to freeze–thaw cycles than the ordinary one.

5. Microscopic Mechanism of Composite-Cemented Soil

5.1. SEM Tests

The samples of ordinary and composite-cemented soil (cured for 7, 28, and 60 d) that were crushed in the UCS tests were reserved and then observed through the SEM to compare their microstructures at 3 kx and 10 kx magnifications. The specific microstructures are illustrated in Figures 8–13.

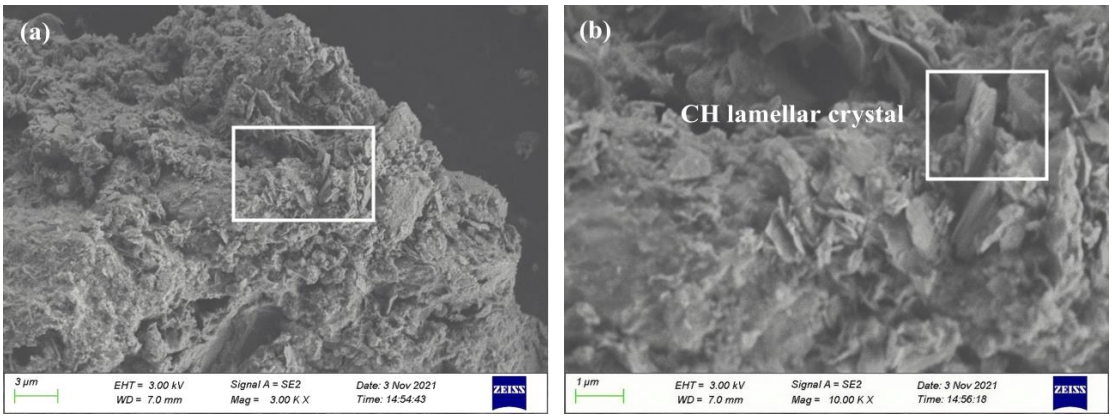


Figure 8. Ordinary-cemented soil cured for 7 d. (**a**) (3.00 kx magnification) and (**b**) (10.00 kx magnification).

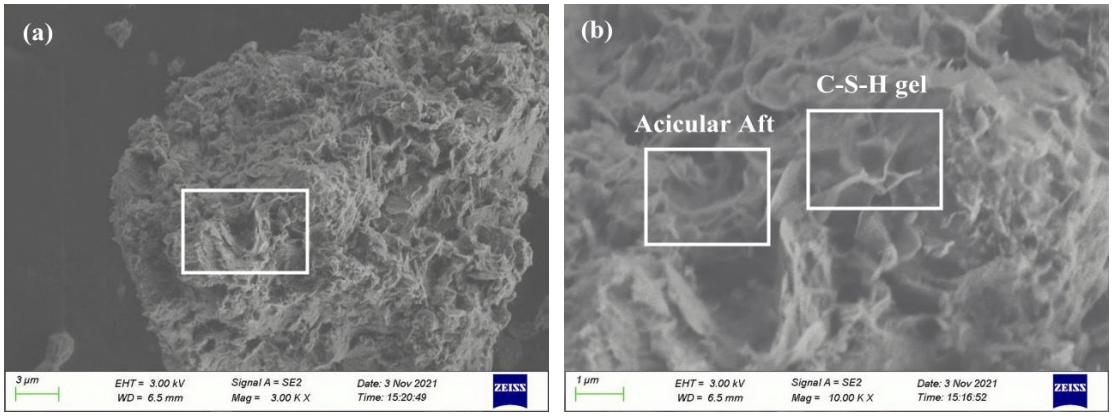


Figure 9. Composite-cemented soil cured for 7 d. (**a**) (3.00 kx magnification) and (**b**) (10.00 kx magnification).

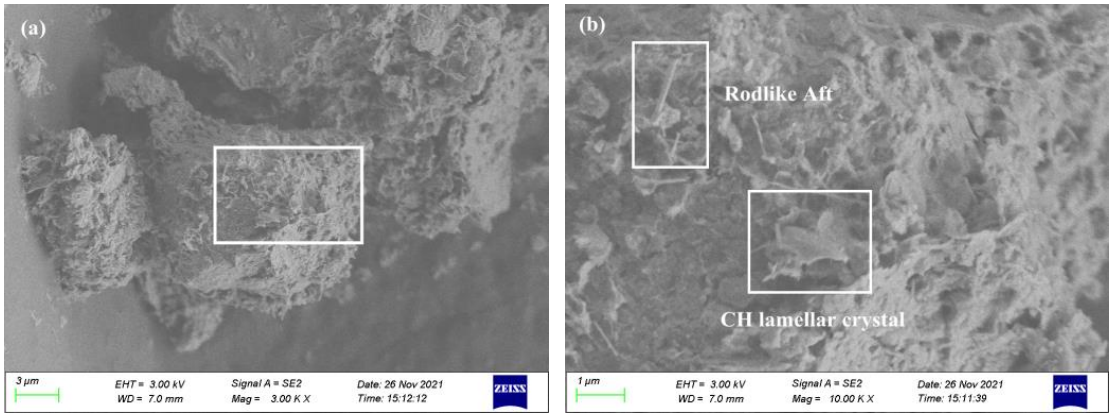


Figure 10. Ordinary-cemented soil cured for 28 d. (**a**) (3.00 kx magnification) and (**b**) (10.00 kx magnification).

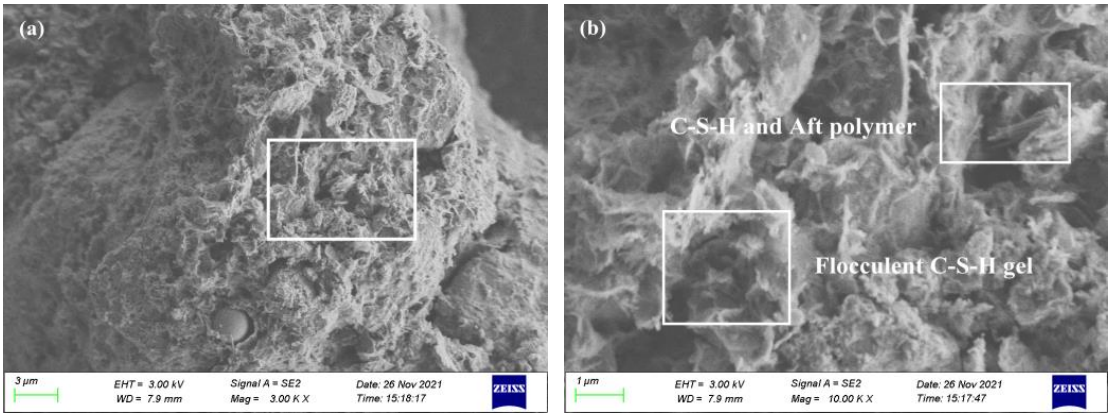


Figure 11. Composite-cemented soil cured for 28 d. (**a**) (3.00 kx magnification) and (**b**) (10.00 kx magnification).

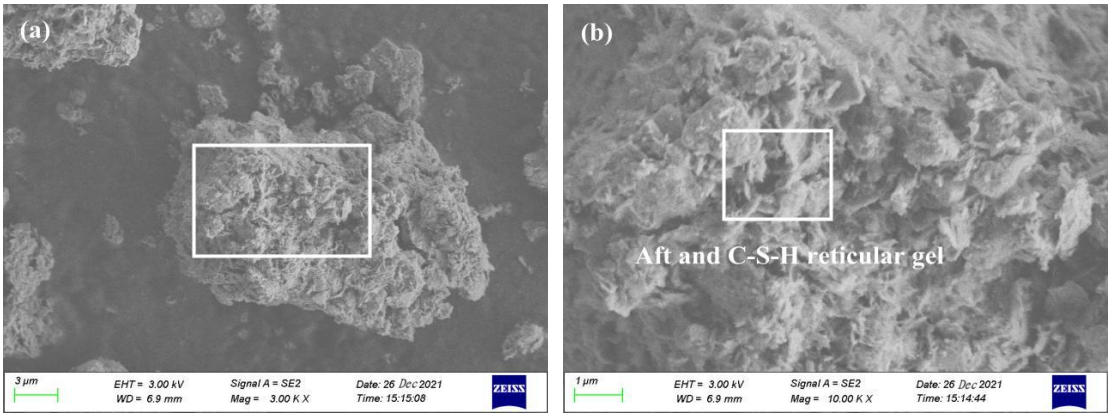


Figure 12. Ordinary-cemented soil cured for 60 d. (**a**) (3.00 kx magnification) and (**b**) (10.00 kx magnification).

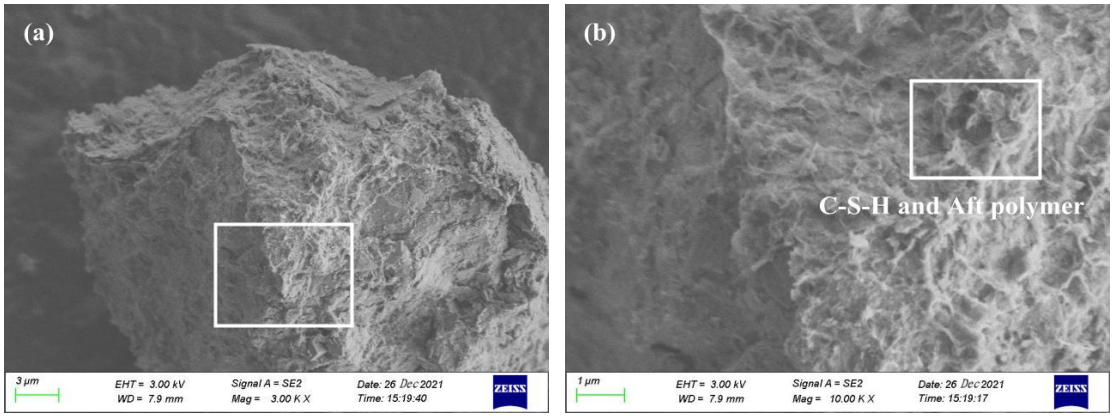


Figure 13. Composite-cemented soil cured for 60 d. (**a**) (3.00 kx magnification) and (**b**) (10.00 kx magnification).

As shown in Figures 8a and 9a, the ordinary- and composite-cemented soil samples both produce a certain amount of hydration products after being cured for 7 d, while they both have rough surfaces and large amounts of pores between soil particles. Combined with Figures 8b and 9b, the two types of cemented soils both contain numerous pores in their microstructures, and certain amounts of bonded materials are found on the surface of soil particles, including slender acicular crystals, lamellar crystals, and reticular colloids. Therefore, it is inferred that the acicular and rodlike structures are Aft crystals, lamellar ones are $Ca(OH)_2$ crystals, and reticular amorphous colloidal structures are C-S-H gel.

It can be seen from Figures 10a and 11a that after being cured for 28 d, the ordinary- and composite-cemented soil samples both produce lots of hydration products, and their soil particles are further cemented. The surface roughness decreases, and the pores reduce, accompanied by the production of plenty of reticular structures in contact with each other. By combining with Figures 10b and 11b, it is evident that the two types of cemented soil have reduced pores in microstructures and hydration products are bonded and wrap the surface of soil particles. More rodlike Aft crystals are generated between soil particles, and a lot of irregular colloidal C-S-H gel is distributed around soil particles to render soil particles to be bonded with each other. As a result, the agglomerated structure is formed initially.

It can be seen from Figures 12a and 13a that the cementation between soil particles and hydration products is further enhanced in both the ordinary- and composite-cemented soil cured for 60 d. It is difficult to distinguish soil particles, the surface roughness further decreases, and a compact structure is formed initially. Combining Figures 12b and 13b indicates that the C-S-H gel formed a reticular structure that covers a large area, which contains cross-distributed short, coarse columnar ettringite crystals. A large quantity of soil particles has been cemented as a whole so that the compactness and integrity of the structure are improved significantly compared with those after a curing period of 7 d. Therefore, the mechanical properties and resistance to wetting–drying and freeze–thaw cycles of the two groups of cemented soils are both strengthened significantly with the increase in the curing period.

A comparison of Figures 8 and 9 shows that the two types of cemented soil after being cured for 7 d both produce a certain amount of hydrates. While compared with the ordinary-cemented soil, more hydrates are generated in the composite-cemented soil, in which a lot of amorphous colloidal C-S-H gel also appears. Correspondingly, the ordinary-cemented soil produces a certain amount of tabular $Ca(OH)_2$ crystals inserted in the gel.

By comparing Figure 10 with Figure 11, the hydration products of the two types of cemented soil cured for 28 d are found to both increase significantly compared with those after a curing period of 7 d. More C-S-H gel is produced in the composite-cemented soil than in the ordinary one. In addition, hydration products are bonded with each other and wrap

soil particles in the composite-cemented soil so that the soil particles are more significantly aggregated, which imparts a more compact structure to the composite-cemented soil.

A comparison of Figures 12 and 13 indicates that after being cured for 60 d, the composite-cemented soil contains more reticular colloidal C-S-H gel than the ordinary one, and this gel wraps large areas of soil particles, which are also connected by Aft crystals that are wrapped by hydrated calcium silicate gel, forming a compact whole. The amount of hydration products also increases in the ordinary-cemented soil, while they fail to fully fill in pores between soil particles. Soil particles in the ordinary-cemented soil are connected by acicular Aft crystals and C-S-H gel, thus, forming blocky structures, which are looser than the structures of the composite-cemented soil, and their strength is also obviously lower. This is because after co-doping of FA and WG in the composite-cemented soil, the catalytic effect of WG on the hydration of cement and the secondary hydration reaction of FA on the hydration products produce more hydration products while facilitating the hydration of cement. Therefore, the composite-cemented soil has a more compact structure and obviously has enhanced mechanical properties and endurance.

By analyzing the hydration process using the SEM, it is evident that the composite-cemented soil contains obviously more hydration products than the ordinary one after any curing period. In addition, the hydrates in the composite-cemented soil play more significant connection and bonding roles for soil particles. Moreover, FA also fills in gaps as micro-aggregates so that the dispersive soil particles form a whole structure that is covered by bonded hydrates, and gaps therein are filled by micro-aggregates.

5.2. XRD Analysis

The composite-cemented soil cured for 28 d was subjected to XRD and energy-dispersive X-ray spectroscopy (EDS) to determine its main phases [29]. The target of the instrument was the Cu target, by using which the diffraction peaks of crystals are mainly measured. The data were processed using the software Jade. Taking the doubled diffraction angle as the abscissa and the peak intensity as the ordinate, the XRD pattern is illustrated in Figure 14. To further determine the correctness of the XRD analysis, an ULTIM MAX 65 energy-dispersive spectrometer (Oxford Instruments, Oxford, UK) was adopted for EDS analysis of the two groups of samples, as shown in Figure 15.

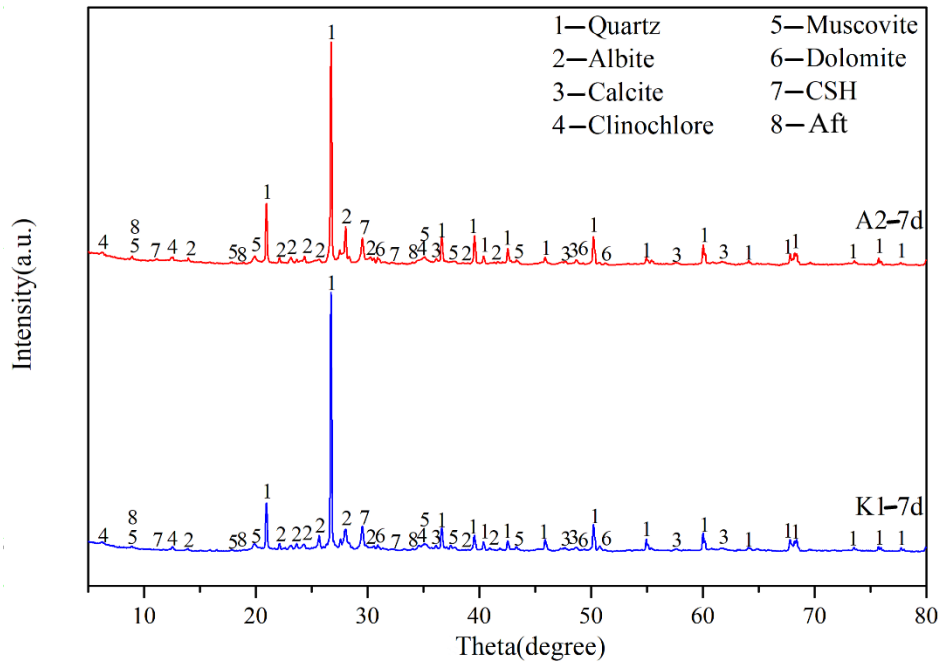


Figure 14. XRD patterns of the ordinary- and composite-cemented soil, cured for 7 d.

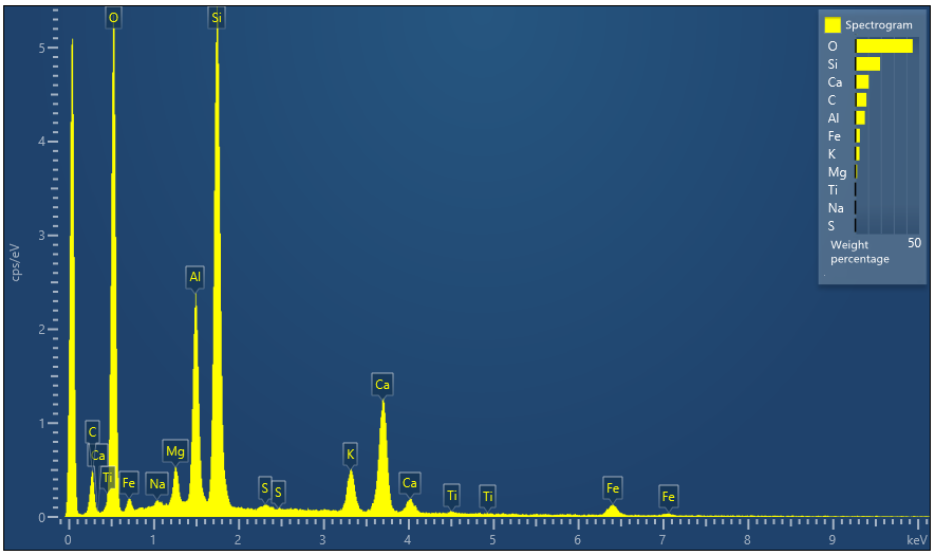


Figure 15. EDS analysis of composite-cemented soil after a curing period of 7 d.

It can be seen from Figure 15 that in addition to quartz, albite, and muscovite intrinsic to the plain soil, the composite-cemented soil cured for 28 d also contains C-S-H and Aft cementing materials, which improve the mechanical properties and endurance of the composite-cemented soil. As shown in Figure 15, the composite-cemented soil cured for 28 d contains relatively higher contents of Si, Al, and Ca, which separately account for 19.44%, 7.48%, and 10.48% of the total mass, respectively. This further verifies the results of XRD analysis.

5.3. Action Mechanism of the FA-WG Composite in Cemented Soil

It can be learned from the above UCS tests and tests on microscopic properties that co-doping of FA and WG can significantly improve both the mechanical properties and degree of microscopic hydration of cemented soil.

FA, as a commonly seen industrial waste, is generally used as a concrete additive. However, due to the low calcium–silicate ratio in the chemical compositions, FA commonly has a high degree of polymerization of [SiO_4] and [AlO_4], so it is difficult to be activated under general conditions.

P. Duxson [30] introduced a polymerization process of materials through alkali activation and proposed that silicate, aluminate, and silicon–aluminate monomers can be produced by dissolving solid particles of FA in an alkali solution. These monomers are polycondensated and rearranged to form silicon–aluminate gel.

Because WG, as a salt of strong alkalinity and weak acidity, can be hydrolyzed, it has strong alkalinity, as expressed below:

$$Na_2O \cdot nSiO_2 + mH_2O \overset{\text{hydrolysis}}{\leftrightarrow} 2NaOH + nSiO_2 \cdot (m\ -1)H_2O \quad (1)$$

Therefore, the alkali activator WG was used here to dissolve low-activity silicon oxide and aluminum oxide in FA and induce further alkali activation for the active reaction of pozzolan in FA. Under the effect of OH^-, FA particles are constantly decomposed to form lots of free SiO_3^{2-} and AlO_2^-. These free acid radical ions are reacted with Ca^{2+} to produce C-S-H and C-A-H gels through polycondensation. As the above reaction continues, the CH content in the cemented soil mixture constantly decreases, thus, promoting the hydration reaction of cement.

Using WG as the activator, the solute $Na_2O \cdot nSiO_2$ was hydrolyzed to produce NaOH and $nSiO_2 \cdot (m-1)H_2O$, and the latter was reacted with Ca^{2+} and OH^- in the mixture to produce C-S-H gel, which promoted the hydrolysis of WG.

$$nSiO_2 \cdot (m-1)H_2O + Ca(OH)_2 = CaO \cdot nSiO_2 \cdot mH_2O \quad (2)$$

By studying the curing mechanism of the composite-cemented soil, the curing process thereof can be roughly revealed, as displayed in Table 8.

Table 8. Curing process of the composite-cemented soil.

Curing Stages	Cement	WG	FA	Soil	Main Hydrates
Initial stage	Hydration reaction begins	Strong alkali and silica gel are produced by hydrolysis of WG.			C-A-H, C-S-H, CH, Aft
Middle stage	Hydration reaction continues	Silica gel aqueous solution produced by hydrolysis is reacted with CH.	WG begins to undergo the pozzolanic reaction with CH under alkali activation.	Reactions of CH with Si and Al activating oxides.	C-S-H, CH, Aft, C-A-H
Middle and late stage	CH is consumed to promote hydration	Water-containing silica gel is consumed to promote hydrolysis of WG.	Under further alkali activation, hydrates of more stable structures are generated.	Stable hydrates are generated after sufficient reactions.	C-S-H, Aft, CH
Late stage	Hydration reaction is basically finished	WG is basically transformed into hydration products	The residual FA further undergoes the hydration reaction under the effect of OH−.	Cementation with hydration products to form high-strength structures.	C-S-H

6. Conclusions

(1) The mixing ratio of cement is critical to the strength development of cemented soil; the mixing ratio of FA exerts an obvious influence on strength development in the middle and late stages; and the mixing ratio of WG only slightly affects the strength. The ratio of cement, FA, and WG of 9%:12%:3% is the optimal engineering mix proportion of the composite-cemented soil. Compared with the ordinary-cemented soil and FA- and WG-cemented soil, the composite-cemented soil has significantly improved compressive load-bearing capacity.

(2) The composite-cemented soil always has a permeability coefficient obviously lower than the ordinary one after any curing period. Despite the mass loss, the composite-cemented soil still has superior endurance to the ordinary one after wetting–drying and freeze–thaw cycles.

(3) Through SEM and XRD analysis, the content of hydration products in the composite-cemented soil is always significantly higher than that in the ordinary one after any curing period. In addition, the bonding action of hydrates on soil particles is more obvious in the composite-cemented soil. The contents of C-S-H gel and Aft crystals in the composite-cemented soil are also apparently higher than those in the ordinary one. Under the alkali activation, FA produces free $SiO_3{}^{2-}$ and AlO^{2-}, which then have polymerization with Ca^{2+} to generate C-S-H and C-A-H gels, further promoting the hydration reaction of cement.

(4) The FA-WG-composite-cemented soil overcomes the large difficulty in backfilling of ultra-deep and ultra-narrow foundation trenches and compensates for the shortcom-

ings of ordinary-cemented soil, including the poor strength, impermeability, and frost resistance. Therefore, it provides a reference for similar engineering.

Author Contributions: Conceptualization, X.D. and N.H.; methodology, X.D. and M.S.; software, M.W.; validation, X.D., N.H. and M.S.; formal analysis, X.D. and M.W.; investigation, M.S.; resources, M.W. and M.S.; data curation, N.H.; writing—original draft preparation, X.D. and M.S.; writing—review and editing, N.H.; visualization, M.S.; supervision, M.W.; project administration, X.D. and M.S; funding acquisition, X.D. All authors have read and agreed to the published version of the manuscript.

Funding: This work was financially supported by the National Key R&D Program of China (grant number: 2018YFB1600100) and the Science and Technology Plan of Shandong Provincial Department of Transportation (grant number: 2021B118).

Institutional Review Board Statement: Not applicable.

Informed Consent Statement: Not applicable.

Data Availability Statement: Not applicable.

Conflicts of Interest: The authors declare that they have no conflict of interest.

References

1. Ter-Martirosyan, Z.G.; Ter-Martirosyan, A.Z.; Vanina, Y.V. Mathematical Computations of Long-Term Settlement and Bearing Capacity of Soil Bases and Foundations near Vertical Excavation Pits. *Axioms* **2022**, *11*, 679. [CrossRef]
2. Chen, J.; Xu, Q.; Luo, X.; Tian, A.; Xu, S.; Tang, Q. Safety Evaluation and Energy Consumption Analysis of Deep Foundation Pit Excavation through Numerical Simulation and In-Site Monitoring. *Energies* **2022**, *15*, 7099. [CrossRef]
3. Rybak, J.; Kongar-Syuryun, C.; Tyulyaeva, Y.; Khayrutdinov, A.M. Creation of Backfill Materials Based on Industrial Waste. *Minerals* **2021**, *11*, 739. [CrossRef]
4. Kongar-Syuryun, C.; Aleksakhin, A.; Khayrutdinov, A.; Tyulyaeva, Y. Research of rheological characteristics of the mixture as a way to create a new backfill material with specified characteristics. *Mater. Today Proc.* **2021**, *38*, 2052–2054. [CrossRef]
5. Połomski, M.; Wiatkowski, M. The Use of Lime for Drainage of Cohesive Soils Built into Hydraulic Engineering Embankments. *Water* **2022**, *14*, 3700. [CrossRef]
6. Sundary, D.; Munirwan, R.; Al-Huda, N. Study of lime addition to sewer sedimentation soil to improve the soil properties for use as construction materials. *J. Phys. Conf. Ser. IOP Publ.* **2021**, *1882*, 012133. [CrossRef]
7. Das, G.; Razakamanantsoa, A.; Herrier, G.; Deneele, D. Influence of wetting fluids on the compressive strength, physicochemical, and pore-structure evolution in lime-treated silty soil subjected to wetting and drying cycles. *Transp. Geotech.* **2022**, *35*, 100798. [CrossRef]
8. Chaiyaput, S.; Arwaedo, N.; Kingnoi, N.; Nghia-Nguyen, T.; Ayawanna, J. Effect of curing conditions on the strength of soil cement. *Case Stud. Constr. Mater.* **2022**, *16*, e01082. [CrossRef]
9. Wang, F.; Li, K.; Liu, Y. Optimal water-cement ratio of cement-stabilized soil. *Constr. Build. Mater.* **2022**, *320*, 126211. [CrossRef]
10. Yu, H.; Yi, Y.; Romagnoli, A.; Tan, W.L. Cement soil stabilization for underground liquid natural gas storage. *Cold Reg. Sci. Technol.* **2022**, *194*, 103438. [CrossRef]
11. OuYang, H.; Dai, G.; Gao, L.; Zhu, W.; Du, S.; Gong, W. Local scour characteristics of monopile foundation and scour protection of cement-improved soil in marine environment-Laboratory and site investigation. *Ocean Eng.* **2022**, *255*, 111443. [CrossRef]
12. Pongsivasathit, S.; Horpibulsuk, S.; Piyaphipat, S. Assessment of mechanical properties of cement stabilized soils. *Case Stud. Constr. Mater.* **2019**, *11*, e00301. [CrossRef]
13. Tianyuan, Z.; Jianming, Z.; Qi, Z.; Shuo, W. Compressive strength of cemented soil in pre-bored grouted planted piles under negative temperature environment. *Transp. Geotech.* **2022**, *35*, 100793. [CrossRef]
14. Zhang, Q.; Zhang, J.; Wang, H.; Zhang, T. Mechanical behavior and constitutive relation of the interface between warm frozen silt and cemented soil. *Transp. Geotech.* **2021**, *30*, 100624. [CrossRef]
15. Shibi, T.; Kamei, T. Effect of freeze–thaw cycles on the strength and physical properties of cement-stabilised soil containing recycled bassanite and coal ash. *Cold Reg. Sci. Technol.* **2014**, *106*, 36–45. [CrossRef]
16. Liang, S.; Chen, J.; Guo, M.; Feng, D.; Liu, L.; Qi, T. Utilization of pretreated municipal solid waste incineration fly ash for cement-stabilized soil. *Waste Manag.* **2020**, *105*, 425–432. [CrossRef]
17. Tao, Z.; Zhang, Y.; Chen, X.; Gu, X. Effects of freeze-thaw cycles on the mechanical properties of cement-fiber composite treated silty clay. *Constr. Build. Mater.* **2022**, *316*, 125867. [CrossRef]
18. Lu, L.; Liu, C.; Qu, S.; Zhang, M. Experimental study on the mechanical and hydraulic behaviour of Fibre-Reinforced cemented soil with fly ash. *Constr. Build. Mater.* **2022**, *321*, 126374. [CrossRef]
19. Pham, T.A.; Koseki, J.; Dias, D. Optimum material ratio for improving the performance of cement-mixed soils. *Transp. Geotech.* **2021**, *28*, 100544. [CrossRef]

20. Wang, F.; Zhao, H.; Ma, J.; Kang, T. Experimental study on the erosion resistance of rubberized cement-soil. *Soils Found.* **2021**, *61*, 734–751. [CrossRef]
21. Liu, J.; Zha, F.; Xu, L.; Kang, B.; Tan, X.; Deng, Y.; Yang, C. Mechanism of stabilized/solidified heavy metal contaminated soils with cement-fly ash based on electrical resistivity measurements. *Measurement* **2019**, *141*, 85–94. [CrossRef]
22. Lu, Y.; Zhang, Y.; Liu, S.; Guo, W.; Xu, F. Mechanical behaviour and permeability of expansive soils mixed with scrap tire rubbers subjected to freeze-thaw cycles. *Cold Reg. Sci. Technol.* **2022**, *199*, 103580. [CrossRef]
23. Kulkarni, P.P.; Mandal, J. Strength evaluation of soil stabilized with nano silica-cement mixes as road construction material. *Constr. Build. Mater.* **2022**, *314*, 125363. [CrossRef]
24. Al-Subari, L.; Ekinci, A.; Aydın, E. The utilization of waste rubber tire powder to improve the mechanical properties of cement-clay 183 composites. *Constr. Build. Mater.* **2021**, *300*, 124306. [CrossRef]
25. Kanty, P.; Rybak, J.; Stefaniuk, D. Some remarks on practical aspects of laboratory testing of deep soil mixing composites achieved in organic soils. *IOP Conf. Ser. Mater. Sci. Eng.* **2017**, *245*, 022018. [CrossRef]
26. Karpisz, I.; Pyda, J.; Cichy, L.; Sobala, D. Study of the effect of cement amount on the soil-cement sample strength. *IOP Conf. Ser. Mater. Sci. Eng.* **2018**, *365*, 042061. [CrossRef]
27. Bagheri, P.; Gratchev, I.; Rybachuk, M. Effects of Xanthan Gum Biopolymer on Soil Mechanical Properties. *Appl. Sci.* **2023**, *13*, 887. [CrossRef]
28. Ministry of Communications of the People's Republic of China. *Test Methods of Materials Stabilized with Inorganic Binders for Highway Engineering*; Ministry of Communications of the People's Republic of China: Beijing, China, 2009; pp. 146–149. (In Chinese)
29. Lindh, P.; Lemenkova, P. Simplex Lattice Design and X-ray Diffraction for Analysis of Soil Structure: A Case of Cement-Stabilised Compacted Tills Reinforced with Steel Slag and Slaked Lime. *Electronics* **2022**, *11*, 3726. [CrossRef]
30. Duxson, P.; Fernández-Jiménez, A.; Provis, J.L.; Lukey, G.C.; Palomo, A.; van Deventer, J.S. Geopolymer technology: The current 190 state of the art. *J. Mater. Sci.* **2007**, *42*, 2917–2933. [CrossRef]

Disclaimer/Publisher's Note: The statements, opinions and data contained in all publications are solely those of the individual author(s) and contributor(s) and not of MDPI and/or the editor(s). MDPI and/or the editor(s) disclaim responsibility for any injury to people or property resulting from any ideas, methods, instructions or products referred to in the content.